Energized oxygen in the magnetotail : Current Sheet Bifurcation from Speiser motion

Don E George[1,2], **Jörg-Micha Jahn**[1,2]

[1]Space Science and Engineering, Southwest Research Institute, San Antonio, Texas, USA.

[2]Department of Physics and Astronomy, University of Texas at San Antonio, San Antonio, Texas, USA.

Key Points:

- Energized dawn-dusk streaming ions exhibit sustained Speiser motion.
- A single population of heavy ions can produce a stable bifurcated current sheet.
- Magnetic reconnection is not required to produce a bifurcated current sheet.

Corresponding author: Don E George, degeorge@swri.edu

Abstract

Oxygen ions can be a major constituent of magnetospheric plasma, yet the role of oxygen in the magnetosphere is often not sufficiently understood. We examine the case of a thinning current sheet prior to the onset of magnetic reconnection. We perform 2.5D PIC simulations of a 3-species system of electrons, protons and heavy ions (O^+). We initiated the simulations using the well-known GEM Challenge configuration. Our approach differs from previous simulations involving heavy ions in two important aspects. First, we initiate the simulations with energized O^+ as opposed to using a thermal population. The energization is based on published in-situ measurements consisting of an initial duskward velocity equivalent to ∼7 KeV. Second, we tracked the particles directly in the simulation rather than performing test particle tracing in post processing.

We show three main results. First, energized dawn-dusk streaming ions exhibit sustained Speiser motion. Second, a single population of heavy ions can produce a stable bifurcated current sheet. Third, magnetic reconnection is not required to produce a bifurcated current sheet.

1 Introduction

1.1 Background

The behavior of individual charged particles in magnetic and electric fields is well understood. The behavior of populations of charged particles in a complex and time variable magnetized plasma environment, such as the case of the Earth's magnetotail, is not well understood.

Singly charged oxygen ions were first measured in the magnetosphere by Shelley et al. (1972). The presence of O^+ in these populations affects basic current sheet behavior and the complex behavior of magnetic reconnection and sub-storm dynamics. The complexities of magnetized plasmas with significant amounts of heavy ions involved in current sheet formation and magnetic reconnection is not well understood. There are many hypotheses explaining the role of O^+ and other heavy ions in thin current sheets. For a full review see Kronberg et al. (2014).

A central concept to magnetic reconnection is the current sheet (CS) that forms at the boundary between two regions in space. In general current sheet thicknesses can vary considerably (half thickness of 650 km to 4700 km) (V. A. Sergeev et al., 1993; Runov

et al., 2006). A CS, in its most basic form, has a centrally peaked current distribution and is referred to as a Harris current sheet (Harris, 1962). Observations show that actual current sheets often have a more complex spatial distribution. A double-peaked or bifurcated current sheet (BCS) differs markedly from the Harris-type current sheet (Thompson et al., 2006). The BCS name is not universally accepted, other names include double-humped, split, double, transient-orbits, or as having two off-center current peaks. Bifurcation is often explained as an actual division of the central current sheet into two separate regions. (Wygant et al., 2005; Israelevich & Ershkovich, 2006; Zelenyĭ et al., 2003; Thompson et al., 2006; Sitnov et al., 2006). In this paper we refer to a BCS only as it is found from dawn to dusk across the magnetotail. We do not refer to island formation or outflow bifurcation as used in magnetic reconnection.

Individual charged particles may become trapped in the magnetic null of a CS. Trapped particles gyro-rotate back and forth across the CS. Once trapped they will be accelerated along the CS by the cross-tail electric field. This guiding-center behavior is best described by the term Speiser Orbits or, when there is little or no duskward velocity component, as "cucumber orbits" (Zelenyĭ et al., 2003). Terms like meandering, non-gyrotropic, non-adiabatic and serpentine are also often used to generically describe this motion. We use the term Speiser motion or Speiser orbits (Speiser, 1965) to describe the motion of individual particles involving repeated crossings of the magnetic null of the CS.

Dalena et al. (2010) show that thermal O^+ and H^+ test particles can become trapped in the current sheet of the magnetotail and assume Speiser orbits. They used test particle simulations to predict that, for a statistical ensemble of concurrent nonadiabatic ion trajectories (i.e. in Speiser orbits), a bifurcated current sheet would be produced. In this paper we demonstrate that this prediction is correct.

1.2 BCS Observations

BCS observations in the magnetotail current sheet are common with half-thickness ranging from 60 km to 4000 km (Cai et al., 2008; Kistler et al., 2005; Dalena et al., 2010; Hoshino et al., 1996; Runov, Nakamura, Baumjohann, Zhang, et al., 2003; Runov et al., 2004; Nakamura et al., 2002; Wygant et al., 2005; Asano et al., 2004). The key indicator of a BCS is the double-humped current distribution centered around the magnetic null of a current sheet. It is considered a deviation from the single peaked Harris model.

The majority of observations of a BCS have scale sizes of hundreds of kilometers, with the overall occurrence of bifurcated sheets among stable (non-flapping) thin (about four ion gyroradii) current sheets being 17% Asano et al. (2005). This corresponds to a scale of a few H^+ gyro-radii. A significant number of BCS encounters show thicknesses of thousands of kilometers. As this half-thickness is not consistent with proton-only CS they are often assumed to be due to heavier ions such as O^+. Recent observations have definitively linked the presence of O^+ to these larger scale bifurcations (Runov et al., 2006).

1.3 BCS Causes

There are several mechanisms for the formation of the double-peaked current sheets (Asano et al., 2004). Presently there are two main categories of possible causes for current sheet bifurcation. First, a wide variety of bulk plasma properties, anisotropies and instabilities are attributed to the production of a BCS:

- Cowley (1978) predicted the existence of a bifurcated current sheet due to a pressure anisotropy where $P_\perp > P_\parallel$. Here a broad region of depressed fields develops at the center of the current sheet. This central region terminates at its outer boundary by a spike in the current density. These spikes on either side of the central region form the bifurcation.
- Sitnov et al. (2003) associated bifurcation with a small ion temperature anisotropy for pancake distributions where $T_\perp > T_\parallel$.
- Splitting of the current sheet (i.e bifurcation) can be due to the nonadiabatic scattering of particles in a strongly curved magnetic field of a thin current sheet (Zelenyĭ et al., 2003).
- A 'bifurcated' current sheet can be explained in terms of a traveling (ion-ion) kink displacement with a single continuous displacement into both hemispheres (Karimabadi et al., 2003).
- Bifurcation of the current density distribution may not depend on an anisotropy of the $T_{ion\parallel} > T_{ion\perp}$, but rather on the anisotropy of the $T_\perp$ alone (Israelevich & Ershkovich, 2008) .
- The source of observed bifurcation to be a result of either a sausage mode or a kink mode propagating dawn to dusk (Runov, Nakamura, Baumjohann, Zhang, et al., 2003).

- Bifurcation can be due to the non-diagonal terms of the pressure tensor and temperature anisotropy (Holland & Chen, 1993).
- Not only bifurcation but also current sheet flapping and reconnection can all be explained as a consequence of various instabilities (Kelvin-Helmholtz, LDHI, and tearing), affecting a Harris current sheet (Ricci et al., 2004).
- Nonlinear development strongly modifies the electron flow velocity in the central region, which induces a bifurcation of the current density (Daughton et al., 2004).
- The main contribution to the current comes from ions, but the bifurcated shape is supported by electrons due to the pressure gradient of their distribution and electric drift terms (Greco et al., 2007).

The second category of causes for bifurcation is magnetic reconnection. Many observations conclude that current sheet bifurcation is a direct product of reconnection (Hoshino et al., 1996; Eastwood et al., 2008; Lottermoser et al., 1998; Karimabadi et al., 2005). There are many instances of bifurcation associated with reconnection outflow (earthward and tailward)(e.g. (Runov, Nakamura, Baumjohann, Treumann, et al., 2003).

However, many observations lead to the conclusion that current sheet bifurcation is independent of magnetic reconnection (Dalena et al., 2010; Runov et al., 2004; Ricci et al., 2004; Runov, Nakamura, Baumjohann, Zhang, et al., 2003; Daughton et al., 2004). Thompson et al. (2006), who argued for association with magnetic reconnection, also indicated that a statistical analysis of identified BCSs show that they can exist well away from the region of magnetic reconnection.

Overall it remains an open question what process leads to the formation of a bifurcated current sheet.

1.4 Oxygen Energization

The dawn-dusk electric field across the magnetotail CS predicts cross-tail ion acceleration as evidenced by a increased dusk-side asymmetry of energized ions (Speiser, 1965; Lyons & Speiser, 1982; Meng et al., 1981). Several investigations of cross-tail electric field acceleration of protons and O^+ have been undertaken resulting in acceleration estimates of >50 keV O^+ (Birn et al., 2001) , 100-200 keV H^+ (Birn et al., 2004)), 20

keV O^+ (Ipavich et al., 1984)), 50-500 keV H^+ (Meng et al., 1981), and 112-157 keV O^+ (Wygant et al., 2005). Without regard to the mechanism, accelerated O^+ in the 12 to 40 keV range has been observed by (Kistler et al., 2005) streaming dawn-dusk in the magnetotail at about 19 RE. Even for a typical quiet-time cross-tail field of 0.5 V/m a thermal O^+ atom could easily gain up to $12keV$ from the cross-tail potential alone streaming only a quarter to halfway across the magnetotail (Baker & Pulkkinen, 1998). See Kronberg et al. (2014) for an overall review of the transport and acceleration of heavy ions in the magnetosphere and tail.

2 Simulations

No previous work has performed kinetic plasma simulations which included energized O+. We performed 3-species 2.5D PIC simulations (explained below) of a thin current sheet. Our simulations build upon similar simulations limited to thermal O+ (Markidis et al., 2011; Karimabadi et al., 2011) and also on work using energized O+ test particles in a magnetic field model (Dalena et al., 2010). We begin with an investigation of the individual and group kinetic behaviors of energized O+ followed by an analysis of bulk current sheet properties. Our simulation culminates in the generation of a sustainable bifurcated current sheet.

2.1 Simulation Methodology

Our simulations begin with a 3-species plasma consisting of electrons, protons and oxygen ions. We base this on the well-known GEM Challenge configuration (Birn et al., 2004). This 2-species configuration served as a baseline for comparisons to previous simulation methods. We modified the plasma by including a thermal oxygen background, adding a small duskward velocity component assuming that energization stems from the cross-tail electric field. This is, of course, not the only source of energization in the magnetotail. The energization of the O^+ has not previously been investigated via kinetic PIC simulations.

2.2 PIC Code

Simulations involving thin current sheets and magnetic reconnection use PIC codes extensively (Hesse et al., 2001; Hesse & Birn, 2004; Hesse et al., 1999; Hesse & Schindler,

2001; Karimabadi et al., 2011; Shay et al., 2007). This investigation uses a 2.5D, fully electromagnetic, Particle-In-Cell (PIC) code (Hesse & Schindler, 2001). The code is structured on a rectangular grid of cells of the Buneman type (Villasenor & Buneman, 1992). Charged particles have a rectangular charge function. They are distributed throughout a rectangular two dimensional grid. Electric and magnetic fields reside in the center of each cell. In a 2.5D simulation the particle positions are calculated in 2D while the particle velocities, electric fields and magnetic fields are calculated in 3D. Hence the designation of 2.5D.

Particles are tracked at sub-grid positions while fields are tracked only at the center of each cell. Bulk simulation properties are also calculated at the center of each cell. Particles and fields are advanced in an alternating fashion via a staggered leapfrog method. Particle positions and particle velocity changes are advanced out of phase by one-half time step. Similarly, magnetic field and currents are advanced out of phase with the electric fields by one-half time step. New particle parameters are calculated from the previous fields by solving the equations of motion. Previous time-step fields are interpolated to the particle sub-grid positions. New field parameters are calculated from particle charge and current densities by solving Maxwells equations. The resulting densities are gathered on the grid vertices. For a detailed explanation see Birdsall and Langdon (1991)).

The time-step is chosen to ensure convergence of the field equations and to meet the Courant-Friedrichs-Lewy (CFL) condition of $C_r = V_{max}\frac{\Delta T}{\Delta X} \leq 1$. Implicit time integration of the fields dampens oscillatory behavior of electromagnetic waves. To ensure charge conservation an iterative "Langdon-Marder" type correction is applied to the electric field values (Bruce Langdon, 1992).

All simulations were performed on a DELL PowerEdge 2900 system with a 3 GHz Quad-Core Intel Xenon 5300 Processor, 48 Gbytes of RAM and 8 TBytes of local hard drive storage. No parallelization was employed. We performed 800 x 400 grid simulations with 10^8 macro-particles run at a typical rate of 200 time-steps (i.e. electron gyroperiods) per computational hour. This resulted in a 6000 time-step computation time of 30 hours.

2.3 Simulation Setup

The simulation region is oriented such that it corresponds to the GSM X-Z plane in the center of Earth's magnetosphere at Y=0. Y corresponds to the GSM out-of-plane direction. Due to the finite size of the simulation box, boundary conditions have been set along all three axis, in keeping with previous PIC simulations. For particles, the X boundaries are periodic. Any particle exiting one side reenters the opposite side with the same velocity vector. The Z boundaries are specularly reflecting. Any particle exiting the +/-Z boundary will reenter at the same location but with the opposite Vz.

Y position is calculated for particles during post-processing. They do not "move" in Y during the simulation. There is, however, an implicit assumption that the boundaries in Y are periodic. This means that for each particle that "exits" along Y another identical particle "reenters" from the opposite side with the same 3D velocity. From the viewpoint of the simulation the particle has not moved.

For the electric and magnetic fields the X boundaries are periodic and continuous. Electric and magnetic fields are zero outside the simulation box. The Z boundaries are simple reflecting boundaries such that an exiting particle will reenter at the same point with the same V_x and V_y but opposibe V_z. This is accounted for in the implicit integration performed in the field calculations. Scaling and normalization of simulation parameters is unitless.

While the 2D box has no Y dimension per se, we track V_y to integrate the Y displacement for each particle during post-processing. The ratio between the electron plasma and gyro frequencies is 5. This establishes the relationship between B_o and n_o. B_o is the peak magnetic field strength in the surrounding bulk plasma. n_o is the initial peak density at the center of the current sheet.

2.4 Initial Conditions

2.4.1 Basic Configuration

Our simulation setup uses the GEM reconnection challenge setup with minor variations to accommodate the larger oxygen gyro-radius. The simulation box is 320 x 160 electron gyro-radii compared to the GEM challenge which used a 128 x 64 box while the computational grid is 800 x 400 nodes. The initial magnetic field configuration repre-

sents an anti-parallel magnetotail. We follow the same $B_x(z)$ magnetic field profile as used in the GEM Challenge. Since our goal was not to "speed up" the simulation we varied from the GEM Challenge by not including a magnetic island perturbation. The GEM Challenge employed a CS half-thickness of 0.5 (λ=0.5) ion (proton) gyro-radii. We initialized the CS half thickness to a value of 1.5 ion (proton) gyro-radii. This variation further avoided the onset of magnetic reconnection. This allowed us more time to study the evolution of the CS.

2.4.2 Mass Ratios

In an ideal simulation the relative masses of the species would reflect physical ratios. This is both computationally prohibitive and unnecessary. Our study uses $m_e/m_{H^+}/m_{O^+}$mass ratios of 1/25/250. Previous kinetic studies have shown that these mass ratios, while not physical, are more than sufficient to study oxygen dynamics.

Kinetic simulations using the GEM challenge with m_p/m_e mass ratios of 25, 180 and 1836 mass ratios had no effect on the larger-scale phenomena (Ricci et al., 2002); the evolution of 2-species reconnection was nearly identical for mi/me of 9, 25, 64, and 100 (Hesse et al., 1999); a ratio of 25 separates the relevant electron physics from the proton physics. We assume that the chosen mass ratios, are sufficient for the study of magnetic reconnection and are also sufficient for the study of the CS prior to reconnection onset.

When comparing mass ratios, Markidis et al. (2011) who used physical masses and Karimabadi et al. (2011) who used reduced mass ratios of 1/10/90, reported separation of scale between the three species for studies of both pre- and post-reconnection evolution. For our study we use $m_e/m_{H^+}/m_{O^+}$mass ratios of 1/25/250, which are therefor more than sufficient to separate the mass effects of the species. Even smaller mass ratios could have been employed to evaluate the kinetic effects studied here, however, we opted for higher ratios in preparation for future studies involving the effect of O^+ on magnetic reconnection.

2.4.3 O^+ Energization

Our O^+ initial conditions are distinctly different from those performed in previous simulation studies which used backgrounds of O^+ in the thermal range (Markidis

et al., 2011; Hesse & Birn, 2004; Karimabadi et al., 2011). What is new in this work is that we "energize" the O^+. This energization is achieved by giving the thermal background a duskward V_y velocity. The initial thermal background of O^+ is energized by the addition of a V_y component. We add this uniform initial velocity in the duskward direction. We found that an initial V_y equivalent to ~25 keV would stabilize to ~7 keV after only a few time-steps. We accept that this impulsive initial push is non-physical, however, it quickly relaxes to a value observed in the magnetotail.

2.5 Test Particles

The PIC simulation is a numerical kinetic treatment of plasma particles. The additional introduction of specific test particles is not needed. The simulation code calculates 2D positions and 3D velocities of 100 million particles. Strictly speaking they are actually macro-particles, yet they behave as individual particles would. Due to the 2D nature of the simulation the Y position is not tracked for particles. We calculate a Y displacement from the V_y at each time-step during post-processing. This Y displacement is in electron gyro-radii as are the X and Z dimensions. The assumption of periodic boundary conditions in the Y direction allows for this. Integration of subsequent Y displacements in this manner allows us to examine the kinetics of individule particles in 3D over time.

3 Simulation Results

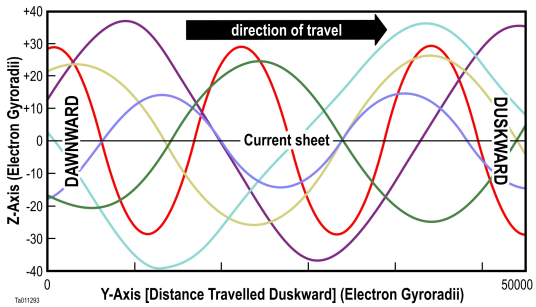

Figure 1. Six representative O^+ ion trajectories along the Y-axis (duskward to the right) following Speiser orbits along +/-Z that cross the current sheet at Z=0, indicated by the horizontal line across the center.

3.1 Individual Test Particle Motion

Figure 1 shows the trajectories of representative O^+ particles. The trajectory of each particle follows a simple sinusoidal curve as it gyro-rotates across the CS while simultaneously moving along +Y duskward.. Thousands of particles (macro-particles) show this same type of trajectory. For clarity only 6 trajectories are shown in Figure 1 while Figure 5 shows 100 representative O^+ particles These sinusoidal tracks indicating Speiser motion as a result of the applied energization.

All O^+ particles accelerated in the simulation exhibit sustained Speiser motion.

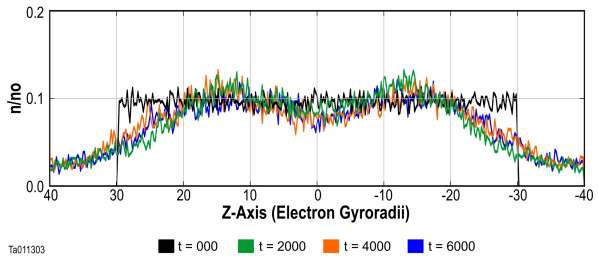

Figure 2. Cross section of $[O^+]$ (density) along Z at X=0 (e^- gyro-radii) for four time-steps (0, 2000, 4000, 6000 e^- gyro-periods). This clearly shows that even though the O^+ ions are moving throughout the Z range, the O^+ density profile (n/n_o) remains consistant over time.

3.2 Density Distribution

We initiated our simulation with a homogeneous density for all three species. H^+ was set to 0.1 n_o over the entire simulation box. O^+ was also set to 0.1 n_o over all X locations but only over the Z range of +/-30 electron gyro-radii. This reduced the heavy ion interaction with the Z boundaries. The e^- distribution was matched to that of the ions to maintain quasi-neutrality of the plasma.

Figure 2 shows the density distribution of O^+ at t=0 and three later timesteps. The distribution remains flat over time, consistent with observations (V. Sergeev et al., 2003) and the evolution of BCS models (Sitnov et al., 2003). More importantly this clearly shows that there is no actual separation of the population into two parts. It is not the particle distribution that is producing the bifurcation. Figure 1 shows the O^+ population moving back and forth across the current sheet. This motion indicates that the gyro-centers

of this population remain on the neutral line. Therefore, the source of bifurcation must have a different cause than the population splitting.

3.3 Current Distribution

The primary indication of a BCS is the double-humped current distribution found along the current sheet. Figure 3 shows a cross section of the O^+ contribution to J_y cut along Z at the center (X=0). First, as it was initialized and then at three later time-steps. This indicates the presence of a BCS with the distinctive double peak with a much lower current in the center. We can attribute the two peaks to a single population of O^+ undergoing gyrorotation along Speiser orbits. This is due to the particle velocity distribution being primarily along the +Y (duskward) axis in the vicinity of both of the current peaks.

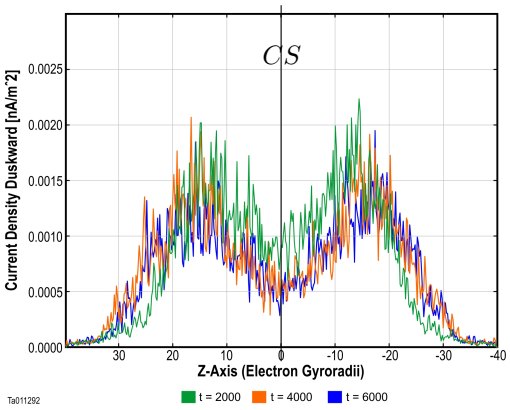

Figure 3. Current flowing in the Y (duskward) direction is calculated by O^+ charge and velocity along the Z axis and integrated over the X axis. A bifurcation in the current centered around the current sheet (Z=0 e^- gyroradii) is clearly evident by the 'double-humped' shape of the current profile. By overlaying the O^+ current density at three timesteps (2000, 4000, 6000 e^- gyroperiods) in the simulation it is evident that the apparent bifurcation is stable and consistent over time.

3.4 Magnetic Field

Figure 4 shows the Z profile of B_x at several timesteps during the simulation, starting from the initial configuration from the GEM challenge Harris Current Sheet.

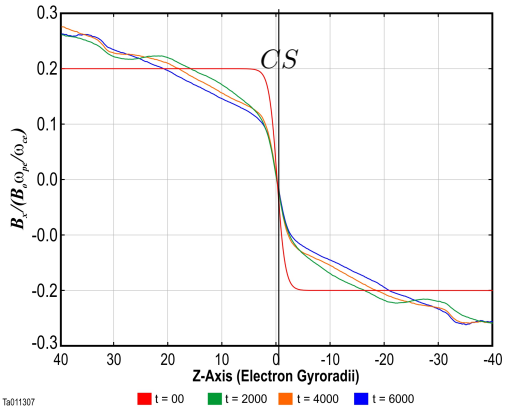

Figure 4. Z Profiles of Bx (for x=400 e^- gyroradii) at: time = 0 (red); at timestep 2000 (e^- gyroperiods) with O^+ present (green); at timestep 4000 (e^- gyroperiods) with O^+ present (orange); timestep 6000 (e^- gyroperiods) with O^+ present (blue).

As time progressesm, the Z-profile of B_x changes. There is some initial flattening of the profile although the basic magnetic configuration remains consistent throughout the simulation. Likewise, throughout the simulation, the magnetic field configuration remains that of a Harris current sheet, even with the presence of a bifurcation.

3.5 Overall System Analysis

While Figures 1 and 3 provide important views of the individual particle behaviors of O^+ plasma, Figure 5 provides a view of their relationship to one another. We show a composite view of the current sheet in 3D. This shows how particle motion and current distribution relate to one another. This composite view reveals the true nature of the bifurcation. We see a bifurcation in the current sheet that is caused by a single "non-bifurcated" population of particles. This bifurcation is not a result of the current sheet splitting, i.e. due to the particle distribution, rather it is a kinetic effect due to a large statistical population all with duskward velocity vectors at the edges of their motion.

The 100 sample trajectories in Figure 5 give a visual representation of the large population moving duskward. Over the entire simulation box there are 100 million O^+ macroparticles. This models a physical population found in the magnetotail. Our sample here depicts a slice at the center (X=0) but is representative across the entire width of the box in X.

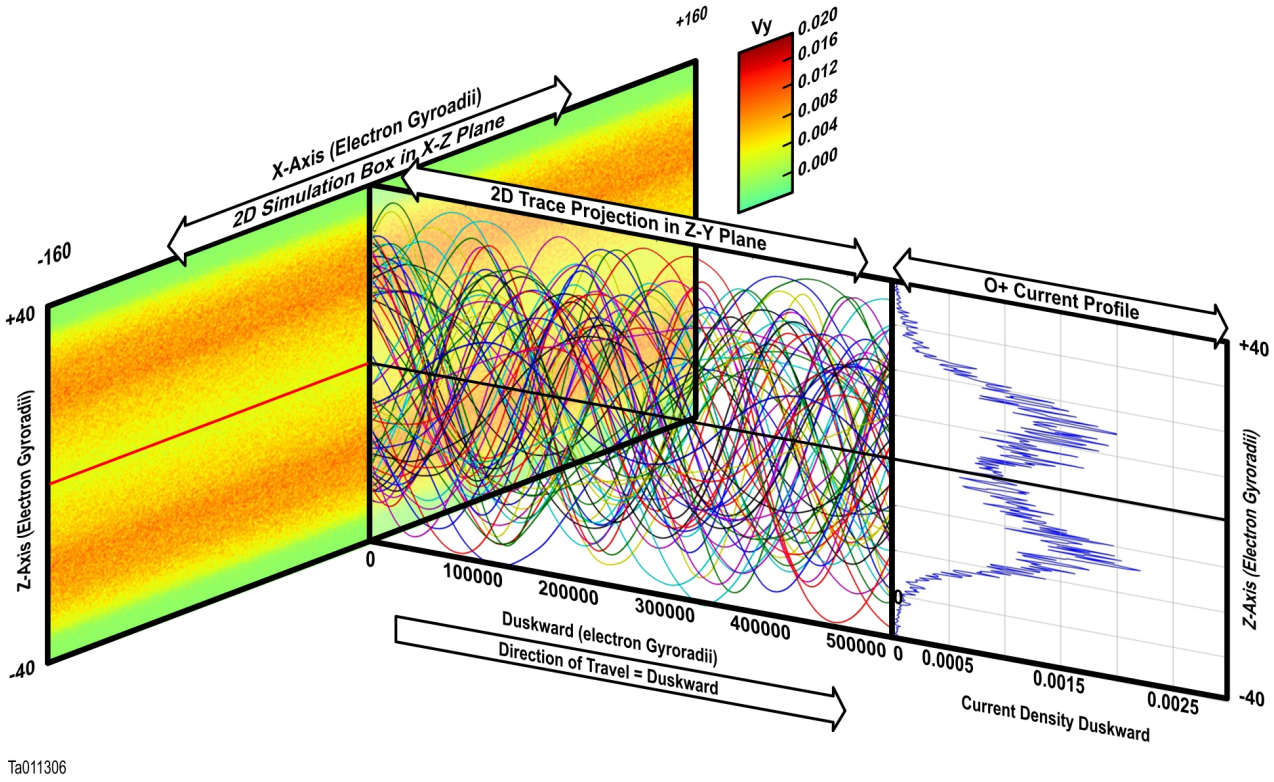

Figure 5. Composite graphic of 1) O^+ velocity in the X-Z plane, 2) 60 trajectory traces of O^+ ions in the Z-Y plane, and 3) the O^+ current profile in Z at X=0 (e^- gyroradii : center) of the simulation box. Taken at timestep 4000 (e^- gyroperiods.)

Each of these many Speiser orbiting trajectories shown is independent of the others. At the same time all these ions are streaming from dawn to dusk (+Y) and gyrorotate in the +/-Z plane. Plotting 100 or even more particles bears no real sign of the bifurcated nature of the current sheet. Only when considering the whole ensemble and adding their velocities to get the current profile the bifurcation is revealed.

Finally we note that the system had not evolved to the point of onset of magnetic reconnection at the end of this simulation. We can conclude that magnetic reconnection is not required for the formation of a BCS.

4 Discussion

In this paper we show three main results. First, energized O^+ accelerated duskward exhibits sustained Speiser motion along the current sheet. Second, a single population

of heavy ions can produce a stable bifurcated current sheet. Third, magnetic reconnection is not required to produce a bifurcated current sheet.

In our simulations bifurcation of a current sheet is purely a result of the kinetic behavior of individual particles. These particles form a single population as opposed to two spatially separate populations. The key to bifurcation is the statistical behavior of a large single population taken as a whole causing a bifurcated current density. The following sequence describes the mechanism. Thermal O^+ ions **of ionospheric origin** migrate into the region near the current sheet. Some ions become trapped around the current sheet magnetic null. Once trapped the cross-tail potential accelerates them from pure gyro-motion to duskward streaming Speiser orbits. As the ions become increasingly energized they continue to gyro-rotate in the magnetic field surrounding the null. The opposing directions of the magnetic field lines combines with the duskward acceleration. This naturally moves the ions towards the null no matter which side they are on. They follow natural kinetic paths referred to as a Speiser orbits. A single, statistically significant, population of Speiser orbiting ions then forms the impression of a bifurcated current sheet by virtue of the ensemble average of Speiser orbits.

On average, for every ion that is crossing the null in one direction there is one crossing in the other direction producing a net particle flux of zero across the CS. Since the net flux of particles crossing the CS is zero, the net current across the magnetic null is also zero.

However this leaves only the parallel velocity components, whose velocities on average all point in the same direction to produce the current distribution. As each ion moves away from the null into the bulk magnetic field, V×B forces turn it back towards the null. This occurs at a distance from the null on the order of the ion gyro-radius. At their furthest distance from the CS (+/-Z) their velocity vector is duskward and parallel to the CS.

The velocity vectors multiplied by the ion charge yields a current. Adding Y velocity components across the CS forms the simulation current profile that peaks on either side of the CS. The particle velocities of ions crossing the CS null are primarily in the Z direction. Thus, rendering the current near the null, the current profile is reduced. Taken together this produces a double-humped current profile which is the very defini-

tion of a bifurcated current sheet. All this occurs without ever splitting the O^+ population into separate populations.

Zelenyĭ et al. (2003) states that Speiser orbits form the basic current of the sheet. Yet, they attribute the bifurcated structure to quasi-adiabatic 'cucumber' orbits. Our work demonstrates that Speiser orbits do produce a bifurcation in the current sheet. Instead, quasi-adiabatic (a.k.a. cucumber or quasi-trapped) orbits (Buchner & Zelenyi, 1989) should be considered a degenerate energy case of Speiser orbits. This means that a cucumber orbit should be a Speiser orbit with a zero or near-zero velocity component along the current sheet. In addition to the PIC simulations performed for this work, we performed simulations of particles in a static 2D CS. These results show that it is common for a trapped particle to assume a cucumber orbit. It also shows that a particle in a cucumber orbit need only be accelerated a tiny fraction of its energy to "assume" a more general Speiser orbit. Such acceleration is easily obtained by the cross-tail electric field.

Comparing a statistical number cucumber orbiting particles to Speiser orbiting particles shows that they could both produce a bifurcated current sheet. This is apparent since both have the same zero net-flux across the CS and both have duskward velocity vectors as they gyro-rotate back towards the CS. A sustained cucumber orbit would be difficult to achieve since even a small acceleration turns it into a Speiser orbit. A sustained statistical population of cucumber orbits would not exist in a physical current sheet due to the presence of the dawn-dusk E-field.

We conclude that it is incorrect to refer to a BCS as two separate currents of a single particle population or as two separate populations. A BCS can be viewed as a purely kinetic phenomenon. It is the result of the superposition of all particles in a Speiser orbiting population onto an underlying Harris type current sheet. This is not to say that there are no secondary effects by other species, CS structure or magnetic reconnection. However these will be explored further in future work. We can argue that lower energy particles gyro-rotate closer to the CS and higher energy particles further away. This produces a bifurcation whose current profile mimics that of the energy distribution. It is obvious that the depth of penetration into the bulk regions outside the CS follow the energy distribution of the ions.

5 Summary

Our work investigated the kinetic behavior of a bifurcated current sheet. We performed 2.5D kinetic PIC simulations of a 3-species plasma consisting of electrons, protons and heavy ions (O^+). A magnetotail-like Harris current sheet configuration was used in following with the GEM Challenge model. To the GEM challenge population of electrons and protons we superimposed a population of thermal O^+ ions. We energized this homogeneous O^+ population with a dusk-ward velocity, equivalent to $\sim$7keV. Individual O^+ particles involved directly in the simulation were tracked throughout the simulations. Post-processing extrapolated the 2D positions and out-of-plane velocities of particles to examine their kinetic behavior in 3D.

Three primary conclusions have been drawn by this investigation. Dawn-dusk streaming O^+ exhibits sustained Speiser motion. A single, statistical, population of heavy ions produces a stable bifurcated current sheet. There is no splitting or division of the ion population. This stable O^+ bifurcated current sheet can exist independently of any magnetic reconnection process.

Previous works have studied the behavior of thermal heavy ions in a current sheet. Energization of these heavy ions is the key to forming a bifurcated current sheet. It is also the key to understanding the nature of the effect of heavy ions on processes in a current sheet. Future work will examine the effect of the energized O^+ population on magnetic reconnection.

Acknowledgments

The authors thank Micheal Hesse, formerly of NASA GSFC, for providing the PIC code used in this work and instruction in its use.

The simulation results used in this study are available at the following repository: https://doi.org/TBD located in https://zenodo.org/communities/plasma-pic-simulation/ .

References

Asano, Y., Mukai, T., Hoshino, M., Saito, Y., Hayakawa, H., & Nagai, T. (2004, May). Statistical study of thin current sheet evolution around substorm onset. *Journal of Geophysical Research (Space Physics)*, *109*(A5), A05213. doi:

10.1029/2004JA010413

Asano, Y., Nakamura, R., Baumjohann, W., Runov, A., Vörös, Z., Volwerk, M., ... Rème, H. (2005). How typical are atypical current sheets? *Geophysical Research Letters*, *32*, issue 3.

Baker, D. N., & Pulkkinen, T. I. (1998). Large-Scale Structure of the Magnetosphere. *Washington DC American Geophysical Union Geophysical Monograph Series*, *105*, 21. doi: 10.1029/GM105p0021

Birdsall, C., & Langdon, A. (1991). *Plasma physics via computer simulation.* Taylor and Francis.

Birn, J., Drake, J. F., Shay, M. A., Rogers, B. N., Denton, R. E., Hesse, M., ... Otto, A. (2001, Mar). Geospace Environmental Modeling (GEM) magnetic reconnection challenge. *Journal of Geophysical Research (Space Physics)*, *106*(A3), 3715-3720. doi: 10.1029/1999JA900449

Birn, J., Thomsen, M., & Hesse, M. (2004, Apr). Acceleration of oxygen ions in the dynamic magnetotail. *Annales Geophysicae*, *22*(4), 1305-1315. doi: 10.5194/angeo-22-1305-2004

Bruce Langdon, A. (1992, July). On enforcing Gauss' law in electromagnetic particle-in-cell codes. *Computer Physics Communications*, *70*, 447-450. doi: 10.1016/0010-4655(92)90105-8

Buchner, J., & Zelenyi, L. M. (1989, Sep). Regular and chaotic charged particle motion in magnetotaillike field reversals. 1. Basic theory of trapped motion. *Journal of Geophysical Research (Space Physics)*, *94*(A9), 11821-11842. doi: 10.1029/JA094iA09p11821

Cai, C. L., Dandouras, I., Rème, H., Cao, J. B., Zhou, G. C., & Parks, G. K. (2008, May). Cluster observations on the thin current sheet in the magnetotail. *Annales Geophysicae*, *26*(4), 929-940. doi: 10.5194/angeo-26-929-2008

Cowley, S. W. H. (1978, Nov). The effect of pressure anisotropy on the equilibrium structure of magnetic current sheets. *Planetary and Space Science*, *26*(11), 1037-1061. doi: 10.1016/0032-0633(78)90028-4

Dalena, S., Greco, A., Zimbardo, G., & Veltri, P. (2010, Mar). Role of oxygen ions in the formation of a bifurcated current sheet in the magnetotail. *Journal of Geophysical Research (Space Physics)*, *115*(A3), A03213. doi: 10.1029/2009JA014710

Daughton, W., Lapenta, G., & Ricci, P. (2004, Sep). Nonlinear Evolution of the Lower-Hybrid Drift Instability in a Current Sheet. *Physical Review Letters*, *93*(10), 105004. doi: 10.1103/PhysRevLett.93.105004

Eastwood, J. P., Brain, D. A., Halekas, J. S., Drake, J. F., Phan, T. D., Øieroset, M., ... Acuña, M. (2008, Jan). Evidence for collisionless magnetic reconnection at Mars. *Geophysical Research Letters*, *35*(2), L02106. doi: 10.1029/2007GL032289

Greco, A., de Bartolo, R., Zimbardo, G., & Veltri, P. (2007, Jun). A three-dimensional kinetic-fluid numerical code to study the equilibrium structure of the magnetotail: The role of electrons in the formation of the bifurcated current sheet. *Journal of Geophysical Research (Space Physics)*, *112*(A6), A06218. doi: 10.1029/2007JA012394

Harris, E. G. (1962, January). On a plasma sheath separating regions of oppositely directed magnetic field. *Il Nuovo Cimento*, *23*, 115-121. doi: 10.1007/BF02733547

Hesse, M., & Birn, J. (2004, February). On the cessation of magnetic reconnection. *Annales Geophysicae*, *22*, 603-612. doi: 10.5194/angeo-22-603-2004

Hesse, M., Birn, J., & Kuznetsova, M. (2001, March). Collisionless magnetic reconnection: Electron processes and transport modeling. *Journal of Geophysical Research (Space Physics)*, *106*, 3721-3736. doi: 10.1029/1999JA001002

Hesse, M., & Schindler, K. (2001, June). The onset of magnetic reconnection in the magnetotail. *Earth, Planets, and Space*, *53*, 645-653. doi: 10.1186/BF03353284

Hesse, M., Schindler, K., Birn, J., & Kuznetsova, M. (1999, May). The diffusion region in collisionless magnetic reconnection. *Physics of Plasmas*, *6*, 1781-1795. doi: 10.1063/1.873436

Holland, D. L., & Chen, J. (1993, September). Self-consistent current sheet structures in the quiet-time magnetotail. *Geophysics Research Letters*, *20*, 1775-1778. doi: 10.1029/93GL01976

Hoshino, M., Nishida, A., Mukai, T., Saito, Y., Yamamoto, T., & Kokubun, S. (1996, November). Structure of plasma sheet in magnetotail: Double-peaked electric current sheet. *Journal of Geophysical Research (Space Physics)*, *101*, 24775-24786. doi: 10.1029/96JA02313

Ipavich, F. M., Galvin, A. B., Gloeckler, G., Hovestadt, D., Klecker, B., & Scholer, M. (1984, May). Energetic (greater than 100 keV) O(+) ions in the plasma sheet. *Geophysics Research Letters*, *11*, 504-507. doi: 10.1029/GL011i005p00504

Israelevich, P. L., & Ershkovich, A. I. (2006, July). Bifurcation of Jovian magnetotail current sheet. *Annales Geophysicae*, *24*, 1479-1481. doi: 10.5194/angeo-24-1479-2006

Israelevich, P. L., & Ershkovich, A. I. (2008, June). Bifurcation of the tail current sheet and ion temperature anisotropy. *Annales Geophysicae*, *26*, 1759-1765. doi: 10.5194/angeo-26-1759-2008

Karimabadi, H., Daughton, W., & Quest, K. B. (2005, March). Antiparallel versus component merging at the magnetopause: Current bifurcation and intermittent reconnection. *Journal of Geophysical Research (Space Physics)*, *110*, A03213. doi: 10.1029/2004JA010750

Karimabadi, H., Pritchett, P. L., Daughton, W., & Krauss-Varban, D. (2003, November). Ion-ion kink instability in the magnetotail: 2. Three-dimensional full particle and hybrid simulations and comparison with observations. *Journal of Geophysical Research (Space Physics)*, *108*, 1401. doi: 10.1029/2003JA010109

Karimabadi, H., Roytershteyn, V., Mouikis, C. G., Kistler, L. M., & Daughton, W. (2011, May). Flushing effect in reconnection: Effects of minority species of oxygen ions. *Planetary and Space Science*, *59*, 526-536. doi: 10.1016/j.pss.2010.07.014

Kistler, L. M., Mouikis, C., MöBius, E., Klecker, B., Sauvaud, J. A., RéMe, H., ... Balogh, A. (2005, June). Contribution of nonadiabatic ions to the cross-tail current in an O^+ dominated thin current sheet. *Journal of Geophysical Research (Space Physics)*, *110*, A06213. doi: 10.1029/2004JA010653

Kronberg, E. A., Ashour-Abdalla, M., Dandouras, I., Delcourt, D. C., Grigorenko, E. E., Kistler, L. M., ... Zelenyi, L. M. (2014, November). Circulation of Heavy Ions and Their Dynamical Effects in the Magnetosphere: Recent Observations and Models. *Space Science Review*, *184*, 173-235. doi: 10.1007/s11214-014-0104-0

Lottermoser, R.-F., Scholer, M., & Matthews, A. P. (1998, March). Ion kinetic ef-

fects in magnetic reconnection: Hybrid simulations. *Journal of Geophysical Research (Space Physics)*, *103*, 4547-4560. doi: 10.1029/97JA01872

Lyons, L. R., & Speiser, T. W. (1982, April). Evidence for current sheet acceleration in the geomagnetic tail. *Journal of Geophysical Research*, *87*, 2276-2286. doi: 10.1029/JA087iA04p02276

Markidis, S., Lapenta, G., Bettarini, L., Goldman, M., Newman, D., & Andersson, L. (2011, September). Kinetic simulations of magnetic reconnection in presence of a background O^+ population. *Journal of Geophysical Research (Space Physics)*, *116*, A00K16. doi: 10.1029/2011JA016429

Meng, C.-I., Lui, A. T. Y., Krimigis, S. M., Ismail, S., & Williams, D. J. (1981, July). Spatial distribution of energetic particles in the distant magnetotail. *Journal of Geophysical Research*, *86*, 5682-5700. doi: 10.1029/JA086iA07p05682

Nakamura, R., Baumjohann, W., Runov, A., Volwerk, M., Zhang, T. L., Klecker, B., ... Frey, H. U. (2002, December). Fast flow during current sheet thinning. *Geophysics Research Letters*, *29*, 2140. doi: 10.1029/2002GL016200

Ricci, P., Lapenta, G., & Brackbill, J. U. (2002, December). GEM reconnection challenge: Implicit kinetic simulations with the physical mass ratio. *Geophysics Research Letters*, *29*, 2088. doi: 10.1029/2002GL015314

Ricci, P., Lapenta, G., & Brackbill, J. U. (2004, March). Structure of the magnetotail current: Kinetic simulation and comparison with satellite observations. *Geophysics Research Letters*, *31*, L06801. doi: 10.1029/2003GL019207

Runov, A., Nakamura, R., Baumjohann, W., Treumann, R. A., Zhang, T. L., Volwerk, M., ... Kistler, L. (2003, June). Current sheet structure near magnetic X-line observed by Cluster. *Geophysics Research Letters*, *30*, 1579. doi: 10.1029/2002GL016730

Runov, A., Nakamura, R., Baumjohann, W., Zhang, T. L., Volwerk, M., Eichelberger, H.-U., & Balogh, A. (2003, January). Cluster observation of a bifurcated current sheet. *Geophysics Research Letters*, *30*, 1036. doi: 10.1029/2002GL016136

Runov, A., Sergeev, V., Nakamura, R., Baumjohann, W., Vörös, Z., Volwerk, M., ... Balogh, A. (2004, July). Properties of a bifurcated current sheet observed on 29 August 2001. *Annales Geophysicae*, *22*, 2535-2540. doi:

10.5194/angeo-22-2535-2004

Runov, A., Sergeev, V. A., Nakamura, R., Baumjohann, W., Apatenkov, S., Asano, Y., ... Balogh, A. (2006, March). Local structure of the magnetotail current sheet: 2001 Cluster observations. *Annales Geophysicae*, *24*, 247-262. doi: 10.5194/angeo-24-247-2006

Sergeev, V., Runov, A., Baumjohann, W., Nakamura, R., Zhang, T. L., Volwerk, M., ... Klecker, B. (2003, March). Current sheet flapping motion and structure observed by Cluster. *Geophysics Research Letters*, *30*, 1327. doi: 10.1029/2002GL016500

Sergeev, V. A., Mitchell, D. G., Russell, C. T., & Williams, D. J. (1993, October). Structure of the tail plasma/current sheet at ˜11 R_E and its changes in the course of a substorm. *Journal of Geophysical Research*, *98*, 17345-17366. doi: 10.1029/93JA01151

Shay, M. A., Drake, J. F., & Swisdak, M. (2007, October). Two-Scale Structure of the Electron Dissipation Region during Collisionless Magnetic Reconnection. *Physical Review Letters*, *99*(15), 155002. doi: 10.1103/PhysRevLett.99.155002

Shelley, E. G., Johnson, R. G., & Sharp, R. D. (1972). Satellite observations of energetic heavy ions during a geomagnetic storm. *Journal of Geophysical Research*, *77*, 6104. doi: 10.1029/JA077i031p06104

Sitnov, M. I., Guzdar, P. N., & Swisdak, M. (2003, July). A model of the bifurcated current sheet. *Geophysics Research Letters*, *30*, 1712. doi: 10.1029/2003GL017218

Sitnov, M. I., Swisdak, M., Guzdar, P. N., & Runov, A. (2006, August). Structure and dynamics of a new class of thin current sheets. *Journal of Geophysical Research (Space Physics)*, *111*, A08204. doi: 10.1029/2005JA011517

Speiser, T. W. (1965, September). Particle Trajectories in Model Current Sheets, 1, Analytical Solutions. *Journal of Geophysical Research*, *70*, 4219-4226. doi: 10.1029/JZ070i017p04219

Thompson, S. M., Kivelson, M. G., El-Alaoui, M., Balogh, A., RéMe, H., & Kistler, L. M. (2006, March). Bifurcated current sheets: Statistics from Cluster magnetometer measurements. *Journal of Geophysical Research (Space Physics)*, *111*, A03212. doi: 10.1029/2005JA011009

588 Villasenor, J., & Buneman, O. (1992, March). Rigorous charge conservation for local
589 electromagnetic field solvers. *Computer Physics Communications*, *69*, 306-316.
590 doi: 10.1016/0010-4655(92)90169-Y
591 Wygant, J. R., Cattell, C. A., Lysak, R., Song, Y., Dombeck, J., McFadden, J., ...
592 Mouikis, C. (2005, September). Cluster observations of an intense normal
593 component of the electric field at a thin reconnecting current sheet in the tail
594 and its role in the shock-like acceleration of the ion fluid into the separatrix
595 region. *Journal of Geophysical Research (Space Physics)*, *110*, A09206. doi:
596 10.1029/2004JA010708
597 Zelenyĭ, L. M., Malova, H. V., & Popov, V. Y. (2003, September). Splitting of Thin
598 Current Sheets in the Earth's Magnetosphere. *Soviet Journal of Experimental
599 and Theoretical Physics Letters*, *78*, 296-299. doi: 10.1134/1.1625728

Figure.

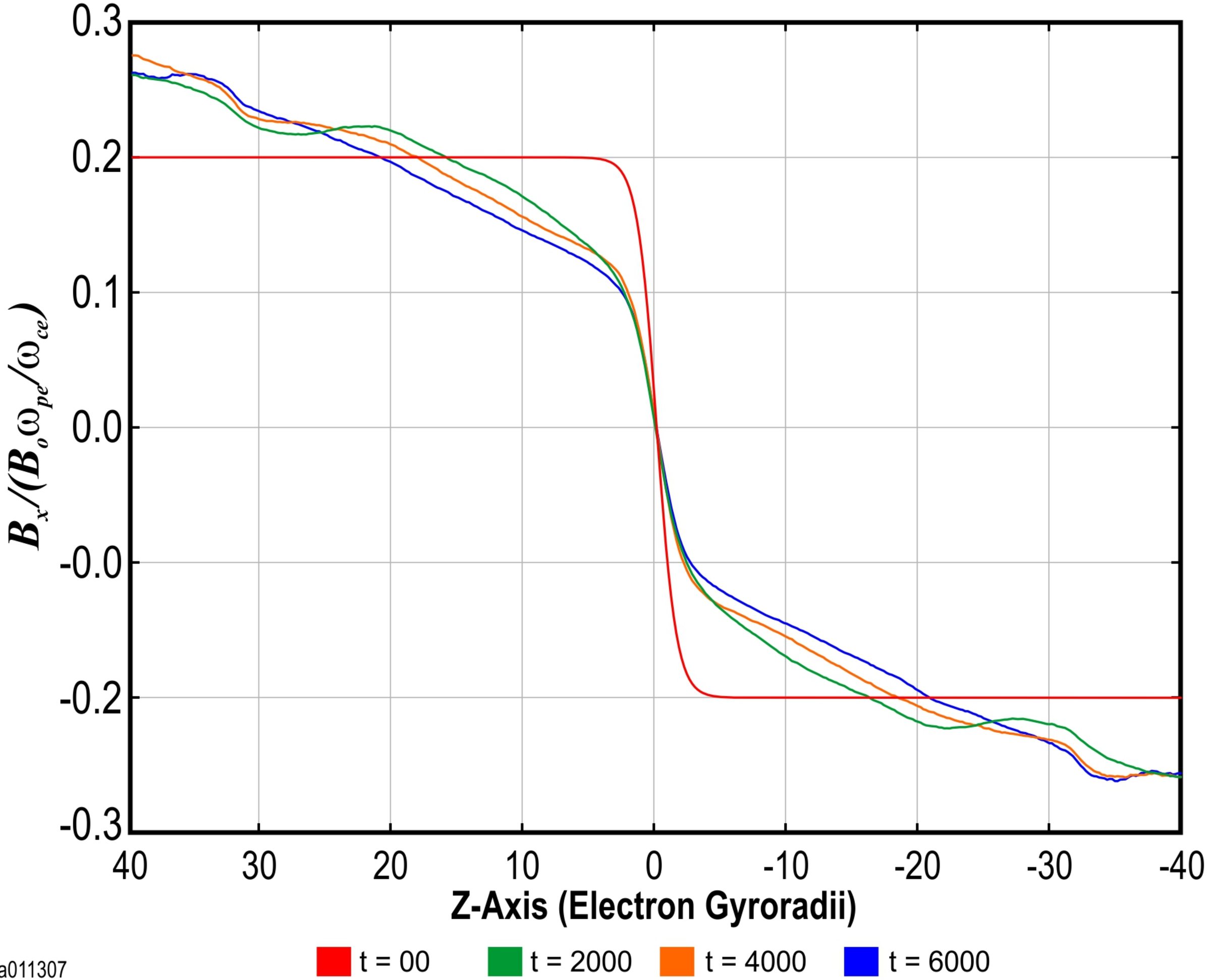
0.3
0.2
0.1
0.0
-0.0
-0.2
-0.3
$B_x/(B_o\omega_{pe}/\omega_{ce})$
40
30
20
10
0
-10
-20
-30
-40
Z-Axis (Electron Gyroradii)
t = 00
t = 2000
t = 4000
t = 6000

Ta011307

Figure.

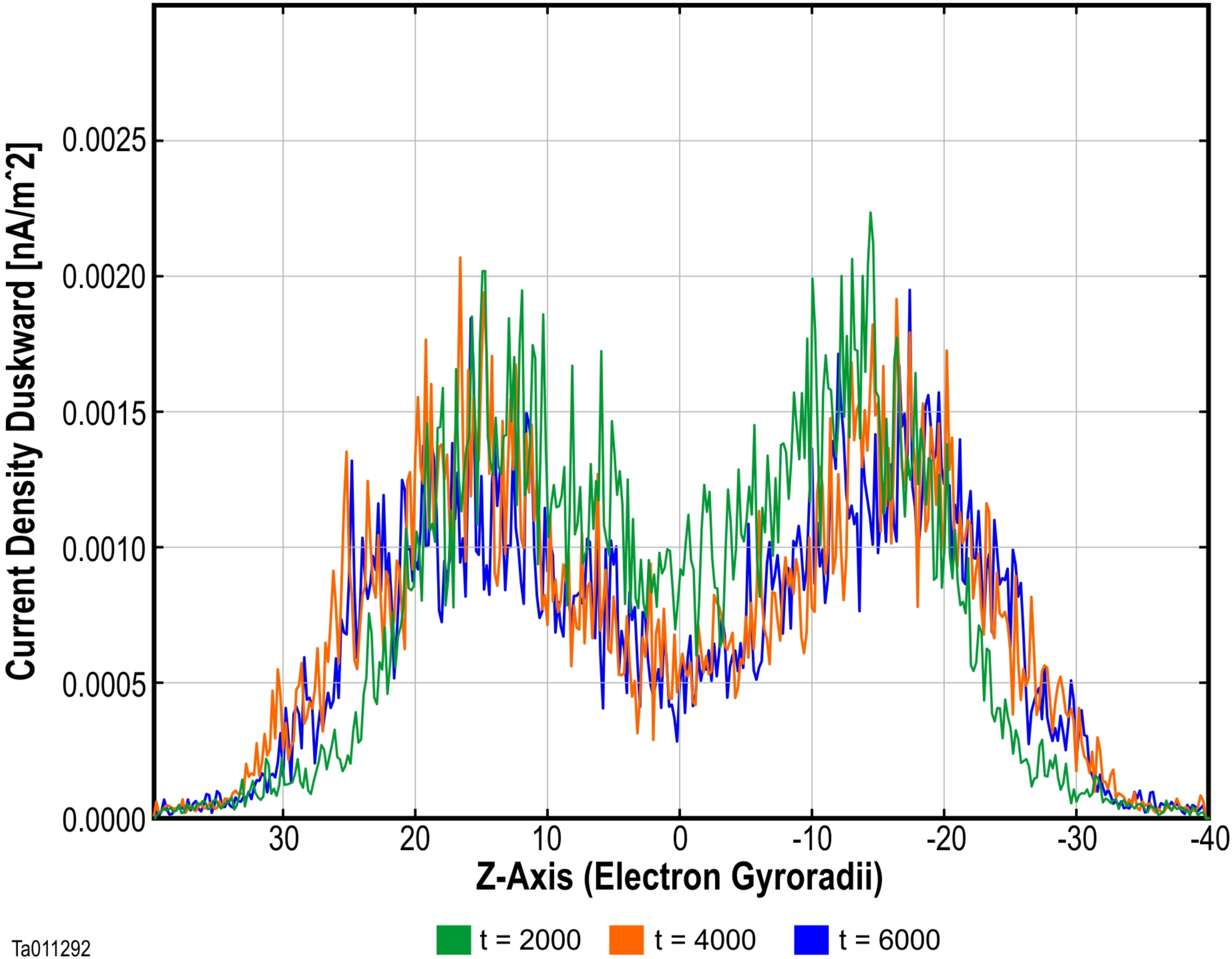
Current Density Duskward [nA/m^2]
0.0025
0.0020
0.0015
0.0010
0.0005
0.0000
30
20
10
0
-10
-20
-30
-40
Z-Axis (Electron Gyroradii)
t = 2000
t = 4000
t = 6000
Ta011292

Figure.

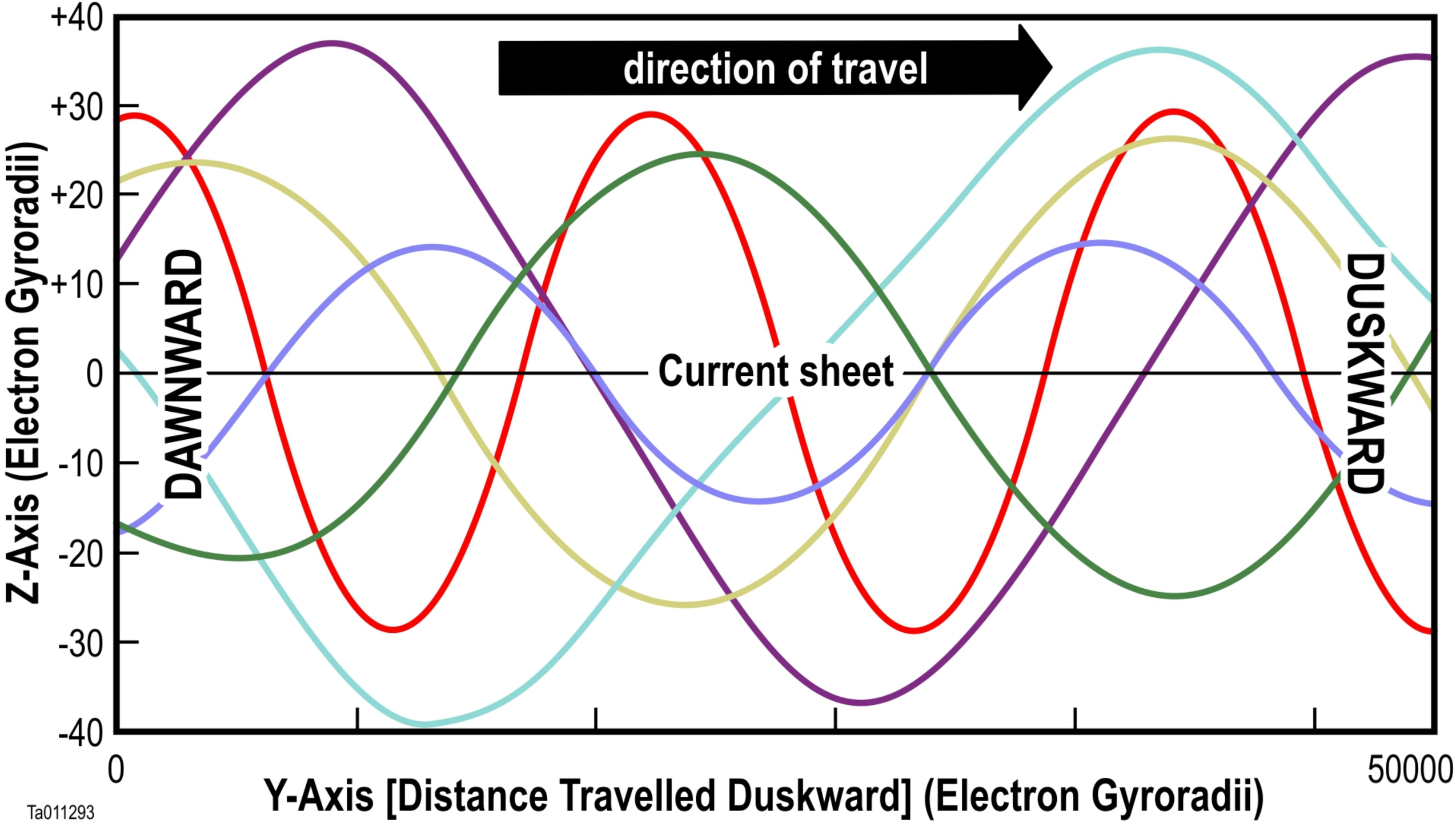
direction of travel
DAWNWARD
DUSKWARD
Current sheet
+40
+30
+20
+10
0
-10
-20
-30
-40
Z-Axis (Electron Gyroradii)
0
50000
Y-Axis [Distance Travelled Duskward] (Electron Gyroradii)
Ta011293

Figure.

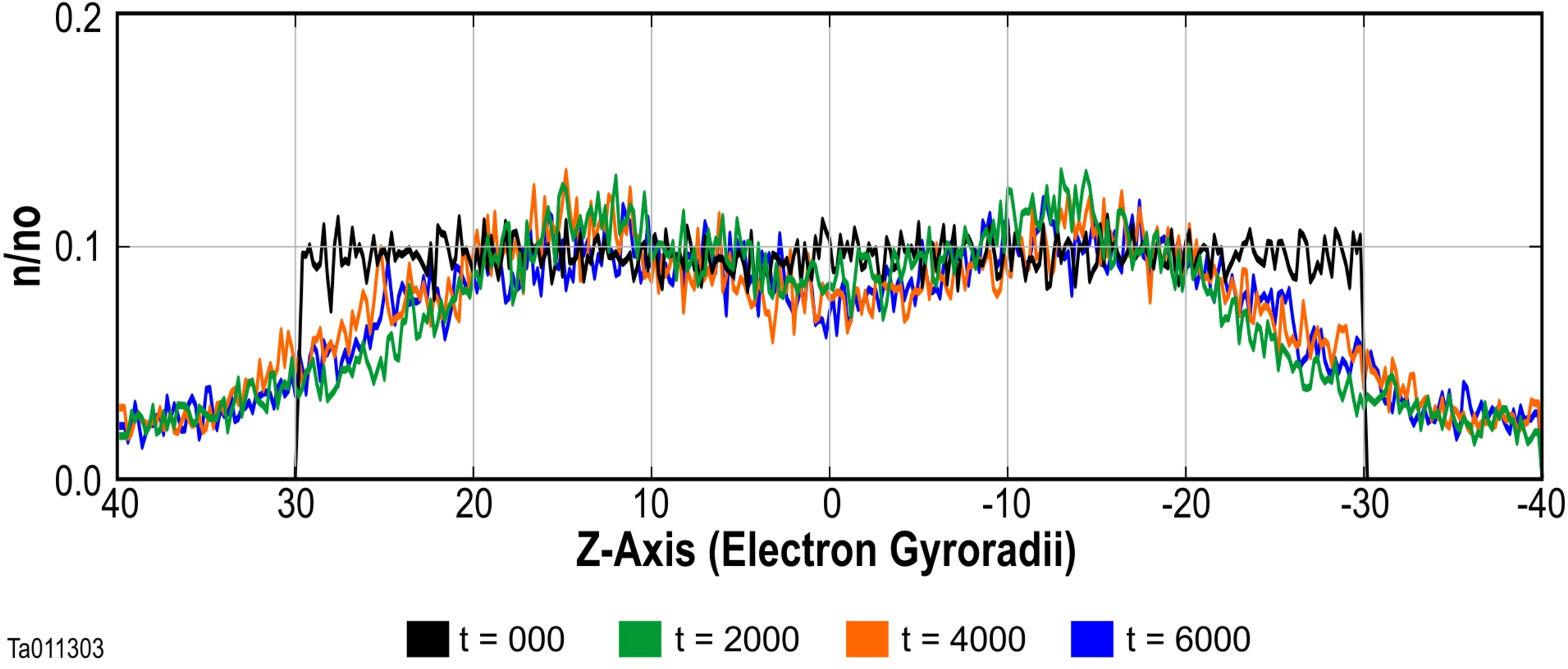
0.2
0.1
0.0
n/no
40
30
20
10
0
-10
-20
-30
-40
Z-Axis (Electron Gyroradii)
t = 000
t = 2000
t = 4000
t = 6000
Ta011303

Figure.

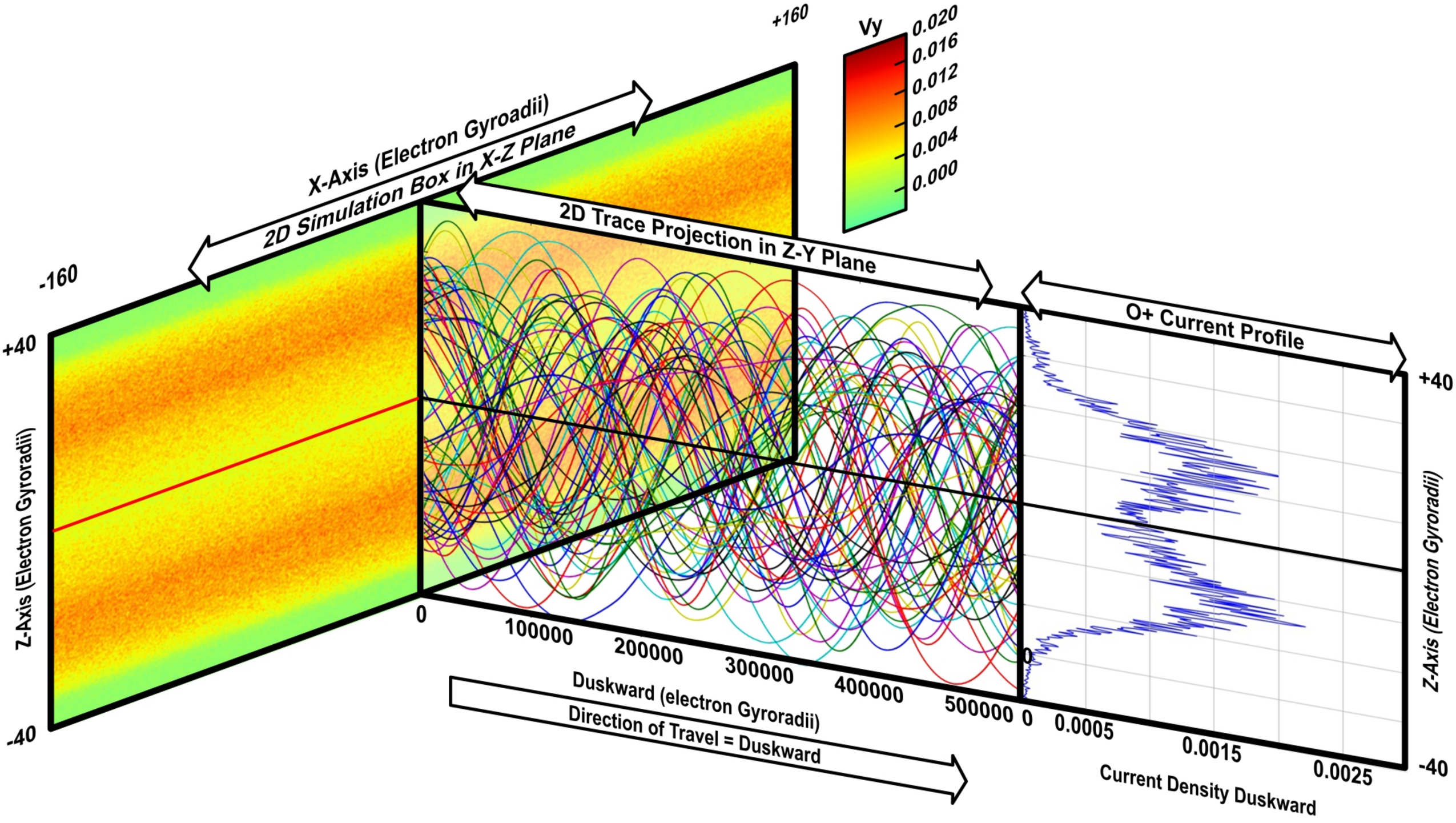
+160
Vy
0.020
0.016
0.012
0.008
0.004
0.000
X-Axis (Electron Gyroadii)
2D Simulation Box in X-Z Plane
2D Trace Projection in Z-Y Plane
O+ Current Profile
-160
+40
Z-Axis (Electron Gyroradii)
-40
0
100000
200000
300000
400000
500000
Duskward (electron Gyroradii)
Direction of Travel = Duskward
0
0.0005
0.0015
0.0025
Current Density Duskward
+40
Z-Axis (Electron Gyroradii)
-40

Ta011306